MRL-R-1133

DTIC FILE COPY

AR-005-250

④

DEPARTMENT OF DEFENCE

DEFENCE SCIENCE AND TECHNOLOGY ORGANISATION

MATERIALS RESEARCH LABORATORY

MELBOURNE, VICTORIA

REPORT

MRL-R-1133

AN EXPLODING FOIL FLYING PLATE GENERATOR

D.D. Richardson, E.D. Northeast and P.F.X. Ryan

DTIC
ELECTE
MAR 0 1 1988
S D
H

DSTO
MELBOURNE

AUGUST 1988

89   3   01   133

AD-A205 157

DEPARTMENT OF DEFENCE

MATERIALS RESEARCH LABORATORY

REPORT

MRL-R-1133

AN EXPLODING FOIL FLYING PLATE GENERATOR

D.D. Richardson, E.D. Northeast and P.F.X. Ryan

ABSTRACT

This paper reports on work done at MRL to generate and use high velocity flying plates. The plates are generated by the pressure from an electrically burst metal foil. We examine some of the important design characteristics of the flying plate generator. We list some possible applications of the method as it applies to shock waves in materials. A discussion of phenomena which have been discovered by using plate impact on a High Explosive to indirectly monitor flying plate velocity is presented.

Approved for Public Release

Table of Contents

AN EXPLODING FOIL PLATE GENERATOR

1. INTRODUCTION

The method by which high velocity flying plates may be generated by electrically exploding a metal foil has been described elsewhere (Logan and others 1977, Weingart 1980, Richardson 1987). A schematic diagram of the apparatus used is shown in Figure 1, while details of the device used are given in Appendix 1. Table 1 provides a summary of the design developed. The (normally polymeric) plate is accelerated when a high voltage (kilovolts) is applied across the metal foil (typically copper or aluminium) bridge. The bridge vaporises in a very short time (about 100 nanoseconds) and generates a very high pressure. This is confined by the tamper material, and pushes out a section of the insulating sheet above the bridge, to form the plate. The pressures from the burst bridge material are high enough to accelerate the plate to velocities normally well above 1 km/s. For larger systems, a velocity of 10 km/s may be possible. In most cases, the plate is allowed to travel across a gap, defined in Figure 1 as a "barrel"*. It then impacts a target material, in which one wishes to apply a high pressure. The actual pressure into the target is a function of the shock properties of both flyer plate and target materials, and the flyer plate velocity at impact. The duration of the pressure wave into the target is a function of the plate thickness and the shock velocity in the flyer plate material. This is a result of rarefactions catching up with the pressure front after travelling twice the shock wave transit time in the plate, when the latter is thin.

An 'Electric Gun' system operating on the same principles has been developed at Lawrence Livermore National Laboratories and used for several years to study shock properties of a range of materials (Weingart 1980, Chau and others 1980). The Livermore work often uses very large bridges, up to 50 mm across, and with correspondingly high

---

* Note that in general the barrel does not serve the same function as a gun barrel. It is there to ensure a suitable gap for the flyer plate to traverse, rather than to provide obturation.

1

electrical energies (kilojoules). In the present work, we have used bridges up to 3 mm in length and width and energies up to 10 joules.

At MRL, we have examined particularly the design parameters of the Flying Plate Generator (FPG) itself. An explosive of known structure and composition will be initiated by an impacting plate of a specific threshold kinetic energy (Voreck and Velicky 1981, Voreck 1983, Mitchell 1985, Thomes and Yactor 1986, Laib 1987). We have used this fact to study changes in plate velocity on impact of an explosive target, as design parameters were varied. It has been found that of particular importance in the FPG design are (i) the tamper material and its attachment, and (ii) the length of the barrel. The latter should ideally be the distance required for the plate to reach its maximum or terminal velocity after acceleration by the bursting bridge. Air or other gases in the region of the barrel will perturb the motion of the plate, and eventually both slow it down and cause it to become unstable in flight.

This technology is being developed to facilitate studies of shock waves in materials. In particular it is expected that it will be possible to (i) measure shock Hugoniots, pressures and pulse duration effects in inert materials, (ii) quantify initiation properties (eg Pop-plots), pressure-duration effects and failure diameter phenomena in reactive materials, and (iii) study shock phenomena such as spallation, multilayer effects and shock wave interactions.

In Section 2 we describe the most important properties of FPGs which we have found by experiment. We will follow this in Section 3 with a discussion of some design modelling. In Section 4 we present an analysis of the properties of FPGs for shock wave studies and describe some of their applications.

2. MEASUREMENTS BASED ON EXPLOSIVE TARGETS

The facilities available for this work have been limited in that direct observation of the motion of the FPG flyer plate has not been possible. It is hoped that in the future we will be able to study the plate motion with a VISAR system (Barker and Hollenbach 1972). Much of the information that we have obtained on our experimental apparatus has been through use of the fact mentioned in the Introduction, that specific explosives have a well-defined minimum plate impact velocity for initiation. By observing changes in initiation threshold energy as a function of changes in component materials, designs and dimensions, (as measured by the energy stored on the capacitor of Figure 1), we have been able to infer many of the design characteristics which are reported here.

2.1 Tamper Effects

The tamper (or anvil), shown in Figure 1, provides a surface against which the expanding gases from the bursting metal foil bridge will push. It prevents the gases from

2

losing energy by expanding into free space on burst. It thus ensures that a significant amount of mechanical work goes into forming and driving the flying plate itself, as the gases from the bursting bridge expand as a result of the deposition of electrical energy into the bridge foil material.

The tamper also serves another purpose. As the bridge expands rapidly at burst, shock waves are formed which will propagate into the surrounding media. The tamper material should be chosen so that it has a large shock 'impedance' mismatch with the bridge foil plasma at burst. This means that most of the energy contained within the shock waves will be reflected at the tamper surface, rather than propagating away through the tamper material, thus adding to the energy available to accelerate the flyer plate.

Figure 2 shows the effects of a range of tamper materials on the electrical energy required to initiate the explosive used. It will be seen that the glass gave the best performance (the lowest stored energy required to initiate the explosive). That is, the glass tamper provided a system which had the greatest efficiency of conversion of the electrical energy into the flyer plate acceleration. Though mica is denser than glass, it produced slightly higher thresholds.

Figure 2 also shows that Teflon tampers did not tamp as well as glass, but were no better than Kapton ones. Teflon, with a density of 2000 kg/m^3, between the densities of Kapton and glass, might have been expected to give better performance than Kapton. We believe that the reason the Teflon did poorly was the observation that the surface . ..sh was poor compared to the glass or the Kapton. Both the latter materials had a glossy appearance, while the Teflon was dull, and clearly had a rough surface. This allows space for significant expansion of the bursting bridge gases with no useful work done, and therefore would explain the poorer tamping behaviour than expected. Since the thickness of the copper foil used in the bridge was about 5 μm, surface imperfections of dimension greater than 10% of this might be expected to allow significant wasted expansion of the bridge material.

The mica tampers were made by cleaving large sheets, and hence the surface finish was good. The tendency for mica to form thin platelets, however, meant the tampers we used probably had air gaps between mica layers, which were impossible to remove. Such gaps were observed from close examination of the material used. The energy absorbed by these air layers during bridge burst is thought to explain the poorer performance of mica relative to glass than might be expected on density alone.

Figure 3 shows the effect of four thicknesses of a Kapton tamper on the input electrical energy before the explosive could be initiated. The Figure shows that thicker tampers are more efficient. This was expected, as thicker tampers will have greater inertial mass. There is also a reduced chance that rarefactions from the back surface of the tamper will affect performance in this case. Simple models, such as that of Gurney (Jones, Kennedy and Bertholf 1980) also support the need for a thick tamper.

From these results we conclude that the tamper should be a dense material, and much thicker than the flying plate material. It must also be an insulator, of course. The tamper should have a smooth surface with the size of imperfections being much smaller than the bridge thickness.

2.2 The Barrel

The barrel, shown schematically in Figure 1, is a vital component of the FPG. Its main purpose is to provide a gap across which the flying plate can be accelerated. Without it, the plate would have very low kinetic energy on impact with the target, and very low pressures would be generated in the target. The length of the barrel determines the distance the plate moves through before impact on the target. We will show that careful choice of the length is important for efficient operation of the FPG.

2.2.1 Barrel Diameter

Recalling that the barrel in the FPG is not normally obturating like a true gun barrel, the diameter of the barrel may, or may not be important, depending on its value. In most of our work, we have used diameters which are larger than (greater than 1.5 times) the width of the bridge. In this case, when the bridge is burst, the flyer plate will form from a bubble in the plastic sheet of the flyer plate material. In some instances the bubble will break around the edges to form a flat flying plate. This is the result of the pressures generated at bridge burst exceeding the material strength of the Kapton flyer material. The diameter of the plate formed in this way is thought to be very close in size to the original bridge width, since for thin foil bridges of the type used, edge effects will be small. (Thickness of the foil is at most a few percent of the bridge width.) The advantage of a large diameter barrel is that its placement on the bridge/flyer is not critical.

For barrel diameters which are comparable to the bridge width, the barrel will define the flyer plate diameter, since the flyer plate material will break away at the barrel edges on bridge burst. The plate shape is thus accurately defined, though some simulation work (Stanton and Kennedy 1980) suggests that the flying plate edges may be slowed by interaction with the barrel walls, causing some deviation from plate flatness.

With small barrel diameters there are other complications. The barrel material will mask some of the outer regions of the bridge which vapourise, so these regions will not contribute to the flyer plate acceleration. The plate will therefore generally be smaller in size. Thus energy will be wasted in that, despite being used to vaporize and expand the bridge in these edge regions, it does not go into the flyer plate. This makes design of the bridge shape itself less critical. We note below (Section 2.3) that the bridge shape must be carefully designed to ensure the most uniform pressure distribution across it. By using the barrel to mask the outer parts of the bridge, the regions of more rapid heating in the bridge do not contribute to the flyer plate, and thus uniform pressure on the flyer is ensured. More careful bridge design is necessary for the large diameter barrel.

It has not been possible to examine barrel diameter effects in detail, but we expect that the energy wasted in the large diameter case in off-axis acceleration of the plate material during bubble formation will be similar in magnitude to the energy lost in the small diameter case due to masking of some of the bridge region. There is some unpublished work by other workers to suggest that this is the case.

4

2.2.2. Barrel Length

Our work on the effects of barrel length   FPG performance revealed some unexpected behaviour which is significant for repeatable operation of the FPG. In all our work large diameter barrels were used.

Figure 4 shows the measured effects of barrel length for one particular bridge size. The Figure shows a plot of stored capacitor energy at which the target explosive just initiated, as a function of barrel length. The interesting effect is the minimum which appears in the curve for a particular barrel length. We have seen this phenomenon for a wide range of bridge dimensions. We will now try to analyse this effect.

The increase in energy for very short barrels can be easily understood. If the barrel is too short, the plate will not have reached terminal ocity by the time it impacts the explosive. The acceleration of the plate will therefore need to be higher for a short barrel so that the plate has reached the threshold velocity for initiating the explosive before impact. If the explosive were removed, the terminal velocity of the plate in this instance would obviously be higher than that at impact. Hence efficiency is down.

The ideal case is when terminal velocity corresponds to the threshold plate kinetic energy for initiation of the explosive. This happens at the minimum in the curve of Figure 4. At this point, terminal velocity is attained just as the plate exits the barrel. The increase in energy beyond this point to achieve the same flyer plate impact velocity has not been previously reported. We are uncertain of the causes of this effect, but speculate that it arises from the plate being slowed down as air builds p in front of the moving plate. The plate is normally moving supersonically, and a shoc wave must build up in the air in front of it. The shock wave will absorb energy from the flyer plate.

Some quantitative analysis of the flyer plate dynamics is possible from our measurements. For a given High Explosive (HE) type, there is a measured minimum plate impact velocity v_x at which the plate will initiate the explosive. Below this velocity the reaction will not propagate. Rather than measuring velocity directly, we measure the threshold total energy E_T into the system, being the energy stored on the capacitor prior to switching. This energy comprises the kinetic energy in the flying plate at impact, E_{KE}, plus additional energies which are absorbed by other elements of the system (such as switch resistance, energy stored in inductance and latent heat for bridge vaporisation), E_o. Thus

$$E_T = E_o + E_{KE}. \tag{1}$$

At the threshold for initiating the explosive, the plate kinetic energy must be

$$E_{KE} = E_x = \frac{1}{2}m{v_x}^2 \tag{2}$$

where m is the flyer plate mass. Thus, knowing v_x for the HE used, an estimate of E_x can be made, based on the diameter and thickness of the flyer plate, and its density. To obtain the diameter of the plate, we assume that it equals the original bridge width.

The energy in excess of that needed to give the flyer the kinetic energy which it requires to detonate the explosive, E_e, is given by

$$E_e = E_T - E_o - E_x \tag{2a}$$

5

(i.e. the total energy given to the capacitor, less that required to form the flyer, E_o, and that required in the best possible case to detonate the explosive, E_x). $E_o = 6.5 \ J$ from a graphical extrapolation of Figure 4 and justified in Appendix 2, and E_x can be calculated from the density (Kapton:1400 kg/m^3) and the velocity of the flyer to be 0.8 J. The mass of the flyer plate is estimated from its density. The diameter of the plate is assumed to be the same as the bridge width. For a 3 mm plate, the mass is 0.25 mg.

Table 2 gives some values for v_x from the literature. The value of v_x depends on the precise system used to measure it - the plate density, thickness and material, the HE morphology, chemistry and density. The data from Table 2 permit a reasonable estimate of v_x to be made which can be used for our analysis.

We illustrate schematically in Figure 5 the calculation we are discussing here. At impact, the plate must have the threshold kinetic energy E_x. Prior to impact, unless the barrel length is less than or equal to that corresponding to the minimum energy of Figure 4, it is assumed that the plate reaches a higher velocity before being slowed down to the impact velocity v_x at the threshold. The excess kinetic energy E_e at the plate's highest velocity is also shown in Figure 5.

We show in Table 3 the results of calculations made on our measurements on 3 mm wide bridge systems (Figure 4). An estimate is shown of the plate kinetic energy based on an extrapolation of the data back to zero barrel length to obtain an estimate of the energy E_o. The estimates are made for the data at barrel lengths greater than or equal to the minimum energy value shown in Figure 4. For the HE used (PETN), v_x =2500 m/s is assumed based on the figure in the literature which was obtained under conditions closest to those pertaining to the present work. Using this figure, an estimate is then given of the excess velocity supplied to the plate in order for it to have the threshold value v_x on impact with the HE. This is a measure of the extra velocity imparted to the plate during acceleration, which has been lost in flight prior to impact. The data are shown as a function of the barrel length. As might be expected from Figure 4, the excess velocity approaches a constant value for relatively long barrels. We are not sure why this is so, but believe that it is the consequence of the setting up of equilibrium shock wave structure in the air surrounding the plate. It may also arise as a result of a precursor shock in the air in front of the plate compressing the HE prior to plate impact, and thereby de-sensitising the HE. Such an effect is reported by Harlan, Rice and Rogers (1981). Since our experiments were done with an explosive powder compressed to about 90% of Theoretical Maximum Density (TMD), however, it seems unlikely that shock de-sensitisation is a large factor in the interpretation. The effect of air could be studied by looking at systems in vacuum for comparison. We have not attempted this.

The maximum velocity shown in the last column of Table 3 is the greatest velocity that the flyer could have attained, given the energy requirements to form the flyer, E_o of about 6.5 J. If there had been no target to hit, then it is thought that for the barrel lengths smaller than 0.5 mm, this maximum velocity is the highest reached by the flyer before it has been slowed down losing kinetic energy to surrounding air.

Ultimately, for very long flight distances, the plate motion would become unstable, and at that point there would be a large increase in uncertainty between measurements, as well as a large overall increase in input energy. Though plate motion is highly stable

6

over a considerable range of displacement, our data do show an increase in energy at long barrel lengths. We have not been able to obtain an accurate standard deviation on our measurements in this region but do expect it to be larger than for shorter barrels.

The results shown in Figure 4, and results for smaller bridges, suggest that for repeatability of impact velocity, independent of precise placement of the target material, barrel lengths should be chosen to be greater than the length at the curve minimum. Our results for a range of bridge sizes from 1 to 3 mm, suggest an empirical relationship betweeen the bridge width w and the barrel length at this minimum l_m, of

$$w = 6l_m. \tag{3}$$

Hence a good barrel length would be one which is about one third of the width of the bridge. These results apply only to barrels with diameter much larger than (greater than 1.5 times) bridge width. For small diameter barrels, similar effects may occur, though they have not been studied here.

2.3 Bridge Shape

A detailed study has been performed of the uniformity of heating of a range of bridge geometries during the burst process (Richardson 1984). These studies indicate that bridge corners should be carefully rounded. When this is done, bridge foils will burst without some of the problems identified by other workers (Logan and others 1977). In particular, the more rapid heating found in bridge corners compared with the centre can be significantly reduced.

Unpublished material by workers in the United States has shown that careful design of bridge shape can significantly reduce the energy at which a FPG system will initiate a particular explosive. It is also likely that the more uniform the bridge heating, the flatter will be the flying plate, since it will experience a more uniform pressure distribution across its surface.

As noted above (Section 2.2.1), the barrel diameter in the FPG can influence the uniformity of acceleration of the plate. Small diameter barrels can be used to mask areas of non-uniform heating, but at the cost of some energy efficiency. This inefficiency is less of a concern for large plate systems (probably for bridge widths above 3 mm, and energies above about 10 J). Large bridges for FPGs can be made by simply laminating strips of metal (aluminium or copper) foil onto the flying plate material. The corners of the bridge are then masked by the barrel, ensuring uniform pressure in the flyer plate region, and a well-defined flyer plate diameter.

Edge effects in the formation of the flyer are most likely to be small since the ratio of width to thickness of the bridge is about 100:1. This means that when the bridge bursts it will effectively act like a two-dimensional surface expanding into a three-dimensional space, and the pressure will be constant across the width of the flyer and will act perpendicularly to accelerate it to high velocity. This being the case, the planarity of the flying plate should be very good (less than 5% variation) if the current density in the bridge is reasonably uniform.

7

3. FPG DESIGN

3.1 Circuit

A schematic diagram of the FPG electrical circuit is shown in Figure 6. The circuit is basically a simple series LRC design, with a time dependent resistive element representing the bridge as it bursts. We assume a lumped-element equivalent circuit, that is, we ignore transmission line effects. (For example, for a short pulse with a 50 ns rise time, the wavelength is approximately 60 m, much larger than the stripline length of typically 30 mm.) For long striplines this will not be valid. For our equivalent circuit, Kirchhoff's Rule gives the equation,

$$L\frac{dI}{dt} + I(R + R'(t)) + \frac{1}{C}(\int_o^t I dt + Q_o) = 0. \tag{4}$$

where the circuit effective inductance is L, series resistance (less the bridge) is R, bridge resistance is $R'(t)$, capacitance is C, initial charge is Q_o on the capacitor and the circuit current is I, at time t. Eqn 4 can be solved by a simple 4th order Runge-Kutta process. It can be re-written as a system of two first order equations

$$\frac{dQ}{dt} = I$$

$$L\frac{dI}{dt} + I(R + R'(t)) + \frac{Q}{C} = 0 \tag{5}$$

with the initial condition that

$$Q_o = CV_o \tag{6}$$

for initial voltage V_o on the capacitor.

The circuit parameters apart from the bridge resistance can be measured by performing a ring-down (Figure 7(a)). This is done by replacing the bridge with a low resistance short-circuit, and functioning the system as usual, while monitoring the current flow. The circuit rings with an under-damped oscillation. Given the capacitance, measured independently, the inductance and resistance of the circuit can be inferred from the period and damping of the oscillations (Richardson 1986) as

$$L = \frac{T^2}{C}\left\{4\pi^2 + \left[ln\left(\frac{I_1}{I_2}\right)\right]^2\right\}^{-1} \tag{7}$$

$$R = \frac{2L}{T} \ ln\left(\frac{I_1}{I_2}\right) \tag{8}$$

8

where T is the oscillation period and I_1, I_2 are the peak values of current for the first two positive-going oscillations.

The period T is related to the frequency of oscillation ω by $\omega = \frac{2\pi}{T}$ where

$$\omega = \sqrt{\frac{1}{LC} - \left(\frac{R}{2L}\right)^2}. \tag{9}$$

Typical parameters for one of the MRL designs are $C = 0.2\ \mu F$, $R = 50\ m\Omega$ and $L = 30\ nH$. Careful design for low inductance is required (Richardson 1987).

The reasons for the low inductance requirement can be understood as follows. Depending on its dimensions, the bridge foil is found experimentally to burst within a few hundred nanoseconds of start of rise of current. Figure 7(b) shows a current trace of a bridge burst which is extremely similar to the ringdown of Figure 7(a) except that the oscillation is stopped by the foil exploding and breaking the circuit. The electrical energy deposited into the bridge region creates a dense electrically resistive plasma which expands approximately adiabatically, analogous to a hot gas working against a piston. A significant fraction of the energy in the plasma will be dissipated once it has expanded to 100-200 % of its initial volume. Since flying plate velocities in the region of 4 km/s are observed after a flight of 0.5 mm, and with an initial foil thickness of 5 μm, the time for the foil-plasma to expand to say 15 μm is approximately 50 ns. Hence the total time available for conversion of electrical energy from the circuit into kinetic energy of the flying plate is about 150 ns. Measurements indicate that this time may in fact be as long as 250 ns. This means that any electrical energy deposited in the plasma at later times is lost. Hence the need for a fast, and therefore low inductance, circuit.

In addition to these considerations, it can be shown on simple energetic arguments that the best energy efficiency will be obtained for bridge burst times which occur at close to maximum current in the first ringdown period. The timing of the bridge burst point is a function of the initial rate of rise of current, which is given by

$$\left.\frac{dI}{dt}\right|_{t=0} = \frac{V_o}{L}. \tag{10}$$

Hence this also depends on the inductance.

The burst point also depends on the dimensions of the bridge, through the total energy required to vaporise and expand the bridge material. A compromise between achievable inductance and bridge size can only be adequately determined by experiment, though the above considerations give a rough indication.

We have experimental evidence, however, that for a given bridge size, there is a value for inductance which provides the most efficient design for a particular capacitance. The choice of the capacitance is again a compromise and is determined partly by the energy that must be stored, and partly by the voltage that the system can be designed to withstand. Depending on the energy of the system, and the size of flying plate desired,

9

capacitance may range from a few tenths to a few microfarads. Voltages range from about 4 kV up to 20 kV in most systems. Stored electrical energy can range from less than 1 joule up to 10 or more kJ.

The behaviour of the bridge itself during burst is, of course, complicated. There have been several approaches used in the past to describe the burst. One of the most popular has been to make use of the concept of specific action, which has been applied extensively to exploding wires (Anderson and Neilson 1959, Mitchell 1985). The specific action at burst is defined by Anderson and Neilson (1959) as

$$g_b = \int_0^{t_b} j^2 dt \tag{11}$$

for current density j in the bridge. It is assumed that this specific action is independent of bridge geometry, circuit parameters and applied voltage. Eqn 11 is used to scale experimental action data for modelling of systems which differ from the measured case. (Workers have in some cases (Tucker and Toth 1975) relied on constant current measurements of burst voltage to obtain suitable data for use with eqn 11.)

In the present work, we have taken a more simplistic approach by using time-dependent measurements of bridge burst resistance, $R'(t)$. This involves simply solving eqn 4 with empirical data on bridge burst resistance $R'(t)$. Measured characteristic waveforms have then been fitted by empirical curves for use in eqn 4, greatly simplifying the analysis. This approach was used by Lee (1986) for exploding wires. There is some arbitrariness about this approach, because at present it is not known how the time to burst from start of current varies with circuit parameters and with bridge dimensions. We use our measurements to determine empirically the width, height and post burst behaviour of bridge resistance as a function of bridge size. The time to burst we determine crudely on the basis of the measurements we have done, by extrapolation. A more rigorous analysis of the experimental data will be undertaken at a later date.

Given an empirical, but analytic, form for $R'(t)$ for the bridge, we then model the circuit behaviour using eqns 4 to 6, along similar lines to Lee (1986). We then assume that the peak in $R'(t)$ defines the burst point and use the calculated current density at this point as input data to a simple Tucker-Stanton (1975) type Gurney calculation of the terminal velocity of the flying plate. This assumes that the barrel length is long enough for the plate to have reached terminal velocity on impact with the target. Effects such as those noted in Section 2.2 cannot be modelled at present.

3.2 Switch

The switch is a vital component of the FPG due mainly to the high speed of burst of the metal foil. The switch that is used must close fast enough, and with low enough equivalent impedance, for it not to affect significantly the performance of the circuit. In other words, it must have inductance and capacitance which are small relative to those of the rest of the circuit, and a resistance on switching which goes from very high (i.e. an open switch) to small relative to all other resistances in the circuit (i.e. closed). The resistance must also drop to its low value in times much faster than the rise of current to bridge burst.

10

Eqn 9 shows that the frequency ω of the circuit (with shorted bridge foil) is dependent on the inductance L and capacitance C provided the circuit is under-damped so that $(R/2L)^2$ is much less than $(1/LC)$. In that case, the period is simply $T = 2\pi\sqrt{(LC)}$. If the switch on-state resistance is too high, the circuit will be overdamped and significant energy will be absorbed in the constant resistance elements of the circuit, reducing efficiency.

The requirements on the values of L, R and C are most stringent in small bridge foil systems, since the burst time of the bridge will be of the order of a few hundred nanoseconds. For large bridge designs, the burst time is relatively long – up to a few microseconds – and the width of the burst resistance versus time curve is greater, and hence switching times can be slower. This means that the rate of drop of switch resistance can be relaxed, and the required on-state resistance can be higher. The term $(R/2L)^2$ in eqn 9 can be increased as long as $(1/LC)$ is increased more rapidly (i.e. the capacitance and inductance of the circuit are decreased).

Several switch types have been investigated for their suitability for use in FPGs. The simplest conceptual type is the air-filled spark gap, where an air gap between two conductors breaks down as a result of either an externally induced voltage or simply due to the large potential difference between the conductors. This type is not believed suitable for any but the largest scale system, since the resistance of such a switch is well over 100 $m\Omega$. Vacuum or gas filled spark gap can be used and normally have lower resistance. They are expensive, however, at the high power ratings required. In general they also have relatively high inductance. An alternative is the shock conduction switch, which is based on the fact that some insulators, such as Kapton (polyimide), become conducting at a certain high pressure (Kapton conducts above 9 GPa, Graham 1980). MRL has developed such a switch in which a copper plate is accelerated into a pair of conductors with Kapton sandwiched between them, creating a very fast, low resistance switch. A disadvantage of such a device is the need to use explosive to drive the copper plate. A third type of switch is a variation on the spark-gap switch, a pull-switch, in which an insulator between the two conductors is mechanically removed when one wishes the device to function. This switch is relatively slow to close and has a relatively slowly falling resistance. It is cheap and simple to make, however, and is quite adequate for larger FPGs. Because of the small gap, typically 0.25 μm, between electrodes, on-state resistance is usually not too high.

4. DISCUSSION

On impact of the FPG-produced plate on the target, a pressure wave will propagate away from the interface. The magnitude p of the pressure wave in the target can be determined from the target material density, its shock velocity and the velocity of the plate at impact. The relation is found from conservation of momentum as

$$p = \rho u_p U \tag{12}$$

where ρ is the density, u_p is the material particle velocity and U is the shock velocity. The particle velocity u_p is given on simple frame of reference grounds as half the flying plate impact velocity.

11

The shock velocity U in the medium is normally determined from the empirically measured 'Shock Hugoniot'. It has been found experimentally that for most materials this is linearly related to the particle velocity as

$$U = c + s u_p \tag{13}$$

where c is the measured speed of sound in the material under shock, and s is an empirical dimensionless constant, typically about 1.5 in value.

Given the constants c and s in eqn 13, the impact pressure can be determined simply from the impact velocity. This makes it possible to study pressures in materials over a wide range, simply by varying the voltage at which the bridge is burst, and hence varying the plate velocity. The relationship linking velocity and circuit voltage can be determined from solving eqn 4 and using the burst point current density in a simple extension of the Gurney model for exploding foil systems, developed by Tucker and Stanton (1975), to estimate plate velocity.

The plate velocity itself can be measured directly, though we have not had the equipment to do so. The most precise way is by the VISAR, a Doppler Interferometer which directly monitors velocity as a function of time for a moving reflective surface. The method was developed by Barker and Hollenbach (1972), and further refined by Hemsing (1983a,b). This technique gives high accuracy and allows monitoring of the full plate velocity history.

Another way to measure the plate motion is by means of high speed photography, though this is more complicated and generally less precise. Because of the time scales involved, and the dimensions of the plate, particularly its small thickness, it is generally difficult to provide external illumination, and such methods often rely on self-light from the bursting bridge foil itself. Streaking methods are normally used. These do not have the wide dynamic range that the VISAR has, though they are useful for a direct measure of plate behaviour.

A simpler technique which lacks precision, but which provides useful data is the Time Of Arrival Method, used by Mitchell (1985). This uses small piezoelectric sensors to detect the arrival of the plate at the target. Given also a measurement of the burst time of the bridge, an estimate can be made of average velocity of the plate. Mitchell (1985) has shown that there is a good correlation between the measured average velocity and the actual impact velocity measured by VISAR. For the same FPG system, there is a simple constant relating the two velocities.

The experimental work of Mitchell (1985) and of Voreck and Velicky (1981) shows a nearly linear relationship between firing voltage and flyer plate impact velocity for a fixed barrel length. This agrees with the simple analysis based on the Gurney model noted above.

The duration of the pressure wave in the target, for a thin plate impact, is dictated by the time it takes for the shock wave to propagate back into the plate to its rear (free) surface. Once the shock wave reaches the rear surface a rarefaction wave moves forward into the plate towards the plate-target interface. The velocity of this rarefaction wave is normally well described by assuming that it is the same as for the shock wave, especially for a thin plate. Hence the duration τ of the pressure wave in the target sample

is just twice the transit time for the shock in the plate, or

$$\tau = \frac{2l_f}{U} \tag{14}$$

where l_f is the flying plate thickness and U is the shock velocity in the plate material. For the systems we have used, the shock velocity is such that the rarefaction catches up with the shock front after only a few flyer plate thicknesses within the target material. For the use of HE targets, as we have done to study the flyer plate behaviour, this means that we must ensure that the HE chosen can be initiated to detonation very close to the surface. Both explosives shown in Table 2 meet this requirement. Among other things, we generally require the HE to have a particle size somewhat smaller than the width of the shock wave.

The FPG can be used to measure Hugoniots. This is done by measuring the transit time of the shock wave through the target material by means either of pressure sensitive gauges in the target, or by observing photographically the transition of the shock wave in materials where the optical properties are pressure dependent. With the use of a pressure measuring gauge at the impact point, pressure can also be determined and a more precise form for the Hugoniot for the material than eqn 13 can be measured. In doing such measurements it is important to ensure that the rarefaction from the rear of the flying plate does not catch up with the shock front before the latter reaches the second gauge measuring the transit time of the shock wave. Detailed calculations show that this can happen for target samples which are thicker than about five times the flying plate thickness, though it depends somewhat on the shock impedances z of target and flyer materials, defined for example by Hayes (1973) as

$$z = \rho U. \tag{15}$$

The FPG method is thus best suited to studying the shock properties of thin films.

5. CONCLUSIONS

This paper reports on an unusual method for generating high velocity flying plates. The results so far using an exploding foil to accelerate a plate show that it is possible to generate plates with good stability, and with reproducible properties. The parametric studies reported here on the design of the Flying Plate Generator indicate that tamper materials should be of high density and much thicker than the flying plate thickness. The tamper also requires a good surface finish and intimate contact with the bridge. The effect of barrel length is such that there is an optimum length for greatest efficiency of conversion from electrical energy into flyer plate kinetic energy, though this is not the best length for reproducible results.

We believe that this method will have great advantages for the study of shock waves in a wide range of materials. The apparatus is relatively compact and except where

13

explosives themselves are to be studied, requires no explosives to generate the shock wave pressures. Because of the almost linear relationship that has been found (by others) between bridge burst voltage and flyer plate velocity after a given displacement (barrel length), it is possible to generate flyer plates over a wide range of velocities, and hence to provide a wide range of pressures into the target. Pressure durations can be altered by the use of different flying plate thicknesses.

In Appendix 1 we have described the design of the FPG used for much of the work reported on here and this is summarised in Table 1. The components and materials used are all commercially available and do not require high tolerances. Such an apparatus is easy to use and uses a minimum of material for each measurement. Only the bridge, tamper and flyer material are expended. Many measurements may be made in rapid succession and the cost per measurement is low, especially if pressure in the target is not monitored.

6. REFERENCES

Anderson G W and Neilson F W (1959), Use of the "Action Integral" in Exploding Wire Studies, in *Exploding Wires*, Eds W G Chace and H K Moore, page 97, Plenum Press, New York.

Barker L M and Hollenbach R E (1972), *J. Appl. Phys.* 43(11), 4669.

Chau H H, Dittbenner G, Hofer W W, Honodel C A, Steinberg D J, Stroud J R, Weingart R C and Lee R S (1980), Electric Gun: A Versatile Tool for High Pressure Shock Wave Research, *Rev. Sci. Instrum.*, 51(12), 1676.

Chen F C (1977), *Introduction to Plasma Physics*, Chapter 1, Plenum Press, New York.

CRC Handbook of Chemistry and Physics, 65th *edition* (1984/1985), ed. R C Weast, CRC Press, Boca Raton, Florida.

Graham R A (1980), Shock-Induced Electrical Switching in Polymeric Films, *Megagauss Physics and Technology*, ed. P J Turchi, Plenum Publishing Corporation.

Harlan J G, Rice J K and Rogers J W (1983), The Role of Air and other Gases in Flyer Plate Initiation of Explosives, *Proc. 7th Int. Symp. on Detonation*, Annapolis MD, 16-19 June 1981.

Hayes D B (1973), Introduction to Stress Wave Phenomena, Sandia Laboratories Report SLA-73-0801, revised 1976.

Hemsing W F (1983a), *Proc. SPIE*, 427, 144.

Hemsing W F (1983b), *Proc. SPIE*, 427, 199.

Jones G E, Kennedy J E and Bertholf L D (1980), *Am. J. Phys*, 48(4), 264.

Laib G (1987), Naval Surface Weapons Center, White Oak, MD, private communication.

Lee R S (1986), An Analytical Model for the Dynamic Resistivity of Exploding Bridgewires, *Proc. 13th Symposium on Explosives and Pyrotechnics*, Hilton Head Island, SC, December 1986.

Logan J D, Lee R S, Weingart R C and Yee K S (1977), Calculation of Heating and Burst Phenomena in Electrically Exploded Foils, *J. Appl. Phys*, 48(2), 621.

Mitchell D E (1985), MC 3926 Interim Development Report, SAND-85-1675.

Richardson D D and Jones D A (1986), A Fast, Low Resistance Switch for Small Slapper Detonators, MRL Report, MRL-R-1030.

Richardson D D (1984), *Engineering Analysis*, 1(4), 195.

Richardson D D (1986), The Effect of Switch Resistance on the Ringdown of a Slapper Detonator Fireset, MRL Report MRL-R-1004.

Richardson D D (1987), The Design of Low Inductance Electrical Circuits, AIP/NZIP Solid State Meeting, Pakatoa, NZ, February 1987.

Stanton P L and Kennedy J E (1980), Minislapper Detonator Development at Sandia, Proc. 4th Explosive Devices Technology Exchange Group, ARRADCOM, Dover NJ.

Thomes J A and Yactor R J (1986), Slapper Parameter Study, LANL Report, in preparation.

Tucker T J and Toth R P (1975), The Electrical Behaviour of Small Exploding Foil Flyer Assemblies, Sandia National Labs Report SAND-75-0445.

Tucker T J and Stanton P L (1975), The Electrical Behaviour of Small Exploding Foil Flyer Assemblies, Sandia Labs Report SAND-75-0041.

Voreck W E (1983), Proc. 7th EDTEG Meeting, Ft Lauderdale, FL.

Voreck W E and Velicky R W (1981), Exploding Foil Shock Sensitivity Test, *Proc. 7th Int. Symp. on Detonation*, Annapolis, MD, 16-19 June.

Weingart R C (1980), Electric Gun: Applications and Potential, Energy and Technology Review, LLNL, UCRL-52000-90-2, 28.

Zentler J M (1982), FUSE: A Simple Simulation Model for a Flyer-Plate Detonator System, LLNL, UCRL-53260.

Table of Symbols

c	measured speed of sound in material under shock
C	capacitance
E_e	excess energy given to the flying plate
E_{KE}	kinetic energy of the flying plate
E_o	minimum energy required to produce a flying plate
E_T	total energy stored in the capacitor
E_x	energy of flying plate required to detonate the explosive
g_b	specific action at burst
$I(t)$	current in the circuit at time, t
j	current density
l_f	flying plate thickness
l_m	barrel length at energy minimum
L	self-inductance of the circuit
L_l	inductance per unit length of a flat cable
p	pressure
Q_o	charge on the capacitor before discharge, i.e. at time $t = 0$
R	circuit time-independent resistance
$R'(t)$	time-dependent resistance, mostly the bridge foil
s	empirical dimensionless constant in shock velocity equation
t	time measured from switching the capacitor
T	period of ringdown
u_p	particle velocity
U	shock velocity
V_o	voltage on the capacitor at time $t = 0$
w	bridge width
z	shock impedance
α	magnitude of exponential damping
μ_o	magnetic permeability of free space
ρ	density
τ	duration of pressure wave in target sample
ω	angular frequency of ringdown

17

APPENDIX 1

A large scale FPG for accelerating thick plates to high velocities in use at MRL

A 0.2 μF oil-filled capacitor supplies the energy to burst the foil. This capacitor is able to deliver up to 10 J of energy when charged to its maximum of 10 kV. A triggered spark-gap switch releases this energy to the bridge circuit.

The bridge foil is soldered to a small disposable stripline consisting of two 20 mm wide, 125 μm thick copper conductors separated by a 75 μm thick sheet of insulating Kapton. The insulator was positioned to prevent shorting of the current through any path other than the desired one through the bridge. Care was taken to ensure good electrical contact of each end of the bridge foil with the conductors.

The conducting strips from this stripline are then, in turn, clamped tightly to a flat cable connected to the terminals of the capacitor.

Both the stripline and cable are made flat to minimise the self-inductance of the circuit, by minimising the area of the circuit loop for magnetic flux to pass through. It can be shown from the Biot-Savart law of magnetic induction that if the conductors have rectangular cross-section of width W and are separated from each other by a distance d, that the inductance per unit length, L_l (in H/m) of such a cable is (ignoring edge effects)

$$L_l = \frac{\mu_o d}{W} \qquad (A1)$$

with $\mu_o = 4\pi \times 10^{-7}$ H/m, d and W in the same dimensions of length. This means that the ratio of width of the conductors to the separation between them should be large. To minimise the inductance of the circuit, so as to maximise the frequency, this ratio should have a value of at least 100 and we use a ratio of 250.

At the frequencies of electrical oscillation encountered in this device, the current penetrates only part-way into a thick conductor, which means that if the conductors in this case were thicker than about 0.2 mm, that extra conductor would not reduce the resistance.

To minimise potential damage to the capacitor from explosive fragments, the cable is 0.5 m long, which gives an inductance for the cable of about 3 nH. The stripline is about 60 mm long and 28 mm wide, with a separation between the conductors of about 200 μm, giving an inductance of about 1 nH. It is thought that the spark-gap switch and the capacitor itself account for the rest of the inductance of the circuit, or about 35 nH.

The resistance and inductance of the circuit are found by ringing the circuit, having a short across the bridge. Measuring the period of the ring directly from a CRO trace and using the exponential decay, we found the inductance to be 38 nH and the resistance to vary between about 75 $m\Omega$ for a voltage of 2.5 kV and 40 to 50 $m\Omega$ for 9 kV, in an inverse hyperbola relationship. The voltage dependence of resistance is due to the spark gap switch having a voltage-dependent resistance.

We summarise the design of the FPG in Table 1.

APPENDIX 2
Thermodynamical basis for E_o

The non kinetic energy contribution E_o for the FPG system described in the present paper can be summarised as follows

$$E_o = E_{sub} + E_{ion} + E_{land\ heating} + E_{res} + E_{shear} \tag{A2}$$

where the terms represent the following quantities:

E_{sub} : energy required to sublime the bridge

E_{ion} : energy required to partially ionize this vapour

$E_{land\ heating}$: energy absorbed by the lands of the foil in the form of their heating

E_{res} : energy lost in the transmission of the pulse through the rest of the circuit

E_{shear} : energy required to shear the kapton to form a flyer

Assuming that significant heating only occurs in the foil, including the bridge and the lands.

The heat energy required to sublime the foil, E_{sub}, can be calculated by breaking it up into heat of fusion, heat of vaporization and the intermediate heating between these two processes

$$E_{sub} = E_{fus} + E_{vap} + E_{heat\ to\ MP} + E_{heat\ to\ BP} \tag{A3}$$

where the quantities are:

E_{fus} : energy required to add to the solid state at the melting point (MP) to change its phase to liquid (heat of fusion ($0.205\ kJ/g$) x mass of the bridge)

E_{vap} : energy required to add to the liquid at the boiling point (BP) to change it to a gas (heat of vaporization ($4.80\ kJ/g$) x mass of bridge)

$E_{heat\ to\ MP}$: heat required to raise the bridge from room temperature to MP (specific heat of the solid ($0.25\overset{\cdot}{o}\ J/g.K$) x mass of bridge x $1060\ K$)

$E_{heat\ to\ BP}$: heat required to raise the bridge from MP to BP (specific heat of liquid ($0.899\ J/g.K$) x mass of bridge x $1484\ K$)

where the specific heats and heats of fusion and vaporization are from the CRC Handbook of Chemistry and Physics (1984/1985). This also assumes that any extra energy supplied

19

tc the bridge to heat it up will go into expansion energy of the gas, and presumably the velocity of the flying plate and therefore should not be included in the calculation for E_o.

The bridge in this calculation has an effective size of 3 x 4 mm, and mass per unit area of 0.038 kg/m^2, which gives it a mass of 0.46 mg. The summation of the terms in equation (A3) then becomes

$$E_{sub} = (0.09 + 2.21 + 0.12 + 0.62) \ J$$
$$= 3.0 \ J.$$

The first ionization energy of copper is 752 kJ/mol, or 11.8 kJ/g (CRC Handbook 1984/1985). However, the bridge vapour does not completely ionize the gas. To do this the temperature of the burst would have to go up to 10^5 K, which it does not do. The model of Zentler (1982) predicts the burst temperature to be 3×10^4 K which, at a pressure at burst time of around 10 GPa, should mean that approximately 20 % of the copper is at first ionization, from the Saha ionization equation (Chen 1977). The ionization energy is thus

$$E_{ion} = (0.2 \times 11.8 \ kJ/g \times 0.46 \ mg)$$
$$= 1.1 \ J.$$

The land areas of the foil will also heat up. Given t at the bridge of the foil vaporizes there must be conduction away of at least some of this heat to the lands and they will probably also be heated by the direct energy pulse. An approximation to the quantity of energy absorbed by this element of the system can be made by assuming that the whole of these land areas rises in temperature to substantially less than the melting temperature of copper. Even if the areas of the lands adjacent to the bridge are on the verge of melting and vaporizing themselves, the areas of the lands further away would not heat up nearly that much.

The lands are about 15 x 15 mm in size each, and are the same material as the bridge. This means that the lands have a total mass of 17.1 mg. If we take this temperature rise to be 200 K then the energy absorbed is

$$E_{land \ heating} = (C_v \times (mass \ of \ lands) \times \Delta T)J$$
$$= 0.255 \ J/g.K \times 17.1 \ mg \times 200 \ K$$
$$= 0.9 \ J.$$

The circuit resistance also absorbs some of the energy of the capacitor. Since the current can be taken as an exponentially damped sinusoid (Richardson 1986)

$$I(t) = I_o \ sin(\omega t) \ e^{-\alpha t} \qquad (A4)$$

where ω is the angular frequency, given in eqn 9, and α is a measure of the speed of damping,

$$\alpha = \frac{R}{2L}.$$

20

The energy absorbed by a resistor in a time varying circuit is

$$E_{res} = \int I^2(t) \, R \, dt \tag{A5}$$

and the square of the current is also a sinusoid, viz

$$\begin{aligned} I^2(t) &= I_o^2 \, sin^2(\omega t) \, e^{-2\alpha t} \\ &= I_o^2 \, \frac{1}{2}\left(1 - cos(2\omega t)\right) \, e^{-2\alpha t}. \end{aligned} \tag{A6}$$

The integral (equation (A5)) can be simply approximated by an average, which in this case is half the square of the maximum current, presuming that the exponential decay is not significant in the time interval of interest. The exact integral is by parts, assuming that the burst of the bridge occurs at one quarter of the period (i.e. integrating from $t = 0$ to $t = T/4 = \pi/2\omega$) which transforms equation (A5) into the following,

$$E_{res} = \frac{1}{2}I_o^2 \, R \left[\frac{1}{2\alpha}\left(-e^{\frac{-\alpha \pi}{\omega}} + 1\right) - \frac{\alpha}{2(\omega^2 - \alpha^2)}\left(e^{\frac{-\alpha\pi}{\omega}} + 1\right)\right]. \tag{A7}$$

The maximum current measured in flyer formation at 8 J of stored capacitor energy is 21 kA, for which the resistance was 45 $m\Omega$, the inductance 37 nH, and the capacitance 0.2 μF. Substituting these values into the equations for α and ω, and then substituting into (A7) gives

$$\begin{aligned} E_{res} &= \frac{1}{2} \, (21 \times 10^3 \, A^2) \times (4.5 \times 10^{-2}\Omega) \times (1.20 \times 10^{-7}s) \\ &= 1.2 \, J. \end{aligned}$$

The shear energy is the only remaining term from equation (A2) left. No figures are available as to the specific energy requirement for the flyers used so far, however it is certain that it is less than 0.1 J based on the shear strengths of similar polymers.

The energy requirement for forming the flyer plate with zero velocity is then the total of these calculated energies, by equation (A2), or approximately 6.3 J, close to the value taken by extrapolation from Figure 4. It must be noted that this energy will change with the voltage of the capacitor, since the current in the circuit changes, meaning that the resistive energy absorption changes. This value calculated does not vary greatly for bursts around 8 J, and in fact the variation can be easily estimated by substituting the new value for the current peak into equation (A7), since the exponential decay accounts for only about 15 % of this value.

If the same calculations are carried out for the smaller bridges used in the work to date, a similar order of correlation results. In the 1 mm bridges used, the minimum energy to fire was measured to be 1.5 J and E_o can be estimated from measurements as 1.0 J. From the above derivation, using a smaller mass of bridge foil and a lower current, the value for E_o is 0.8 J. For the 1.5 mm case, where the minimum burst energy is at 2.6 J, E_o can be calculated as 1.6 J.

21

TABLE 1

Components of the flying plate generator in use at MRL.

Component	Description
Power Supply	Reynolds Industries FS-14 firing capacitor power supply, 0 to 10 kV.
Capacitor	Low inductance Oil-filled 0.2 μF capacitor, Reynolds Industries.
Flat Cable	Copper shim, 125 μm thick. Two lengthss each 50 mm wide, 500 mm long and bolted to the terminals of the capacitor. They sandwich an 80 mm wide strip of polyimide insulator, 75 μm thick, to prevent short circuiting.
Stripline	75 μm, 28 mm wide copper laminated on polyester. Two lengths, 50 and 70 mm long respectively, separated by polyimide insulator, and stuck together in a flat arrangement by double-sided tape. Since one is shorter than the other, there is a gap for the placement of the bridge foil.
Exploding Foil	1/8 oz/ft^2 or 0.038 kg/m^2 (about 5 μm thick) copper laminated on 25 μm thick polyimide (Kapton) supplied by Fortin Industries. Photo-etched to give approximately 15x15 mm lands and a 3x3 mm bridge.
Switch	Triggered spark-gap, part of the FS-14.

TABLE 1
(Continued)

Components of the flying plate generator in use at MRL.

Component	Description
Flying Plate	The 20 μm polyimide upon which the copper foil is laminated. Plate mass, based on a density of 1400 kg/m^3 is approximately 0.25 mg for a 3 mm bridge.
Barrel	Various plastics, such as polythene are used. Any non-conducting material is suitable, as long as the barrel is smoothly cut out from it.
Tamper	Glass, 0.2 mm thick covering about twice the bridge area.

TABLE 2

Threshold impact velocity v_x for small Kapton plates to initiate the explosives shown. Figures quoted are approximate, based on a range of measurements. Plates are generally small in diameter ($< 1\ mm$).

HE	v_x (m/s)	v_x range (m/s)	Ref	Comments
PETN	2500	2300-3100	1	High surface area HE
	2600	2200-2600	2	High surface area HE
	2300	2000-2500	3	Approx 6 mm plates
HNS	2900	2800-5300	2	Fine particle HE at low v_x end.

1. Thomes & Yactor 1986

2. Mitchell 1985

3. Voreck 1983

TABLE 3

Estimates of flyer plate Kinetic Energy for 3 mm width bridges. Also given is estimated maximum velocity of the plates. The data are given for a range of barrel lengths. A value of $v_e = 2500$ m/s is used.

Barrel length (mm)	E_T (J)	$E_T - E_x$ (J)	E_c (J)	Maximum Velocity (m/s)
0.25	$9.3 \pm .2$	8.5	2.0	4600
0.35	$9.4 \pm$?	8.6	2.1	4700
0.5	7 ?	7.0	0.5	3100
0.65	8.7	7.9	1.4	4100
0.8	$8.8 \pm .2$	8.0	1.5	4200
0.9	$8.8 \pm .3$	8.0	1.5	4200
1.0	$9.5 \pm .4$	8.7	2.2	4800
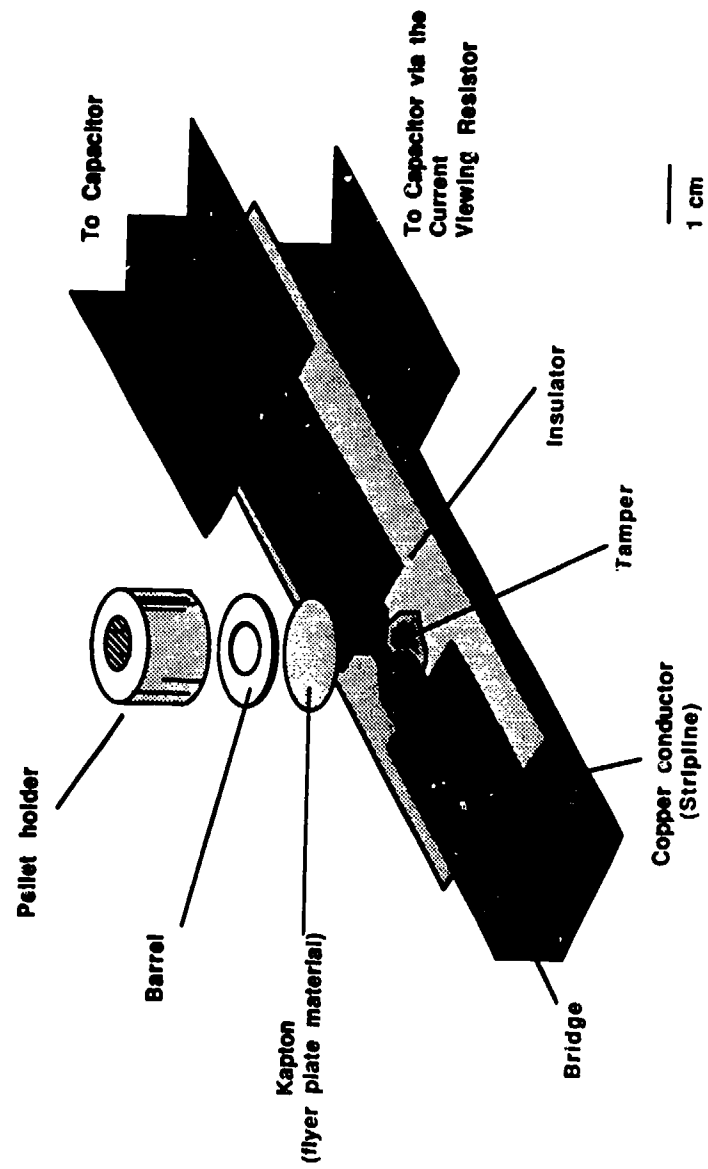
Flying Plate Generator Stripline and Bridge

Pellet holder

Barrel

Kapton
(flyer plate material)

Bridge

Copper conductor
(Stripline)

Tamper

Insulator

To Capacitor

To Capacitor via the
Current
Viewing Resistor

1 cm

Figure 1. A Schematic diagram of the main components of a Flying Plate Generator for shock wave studies.
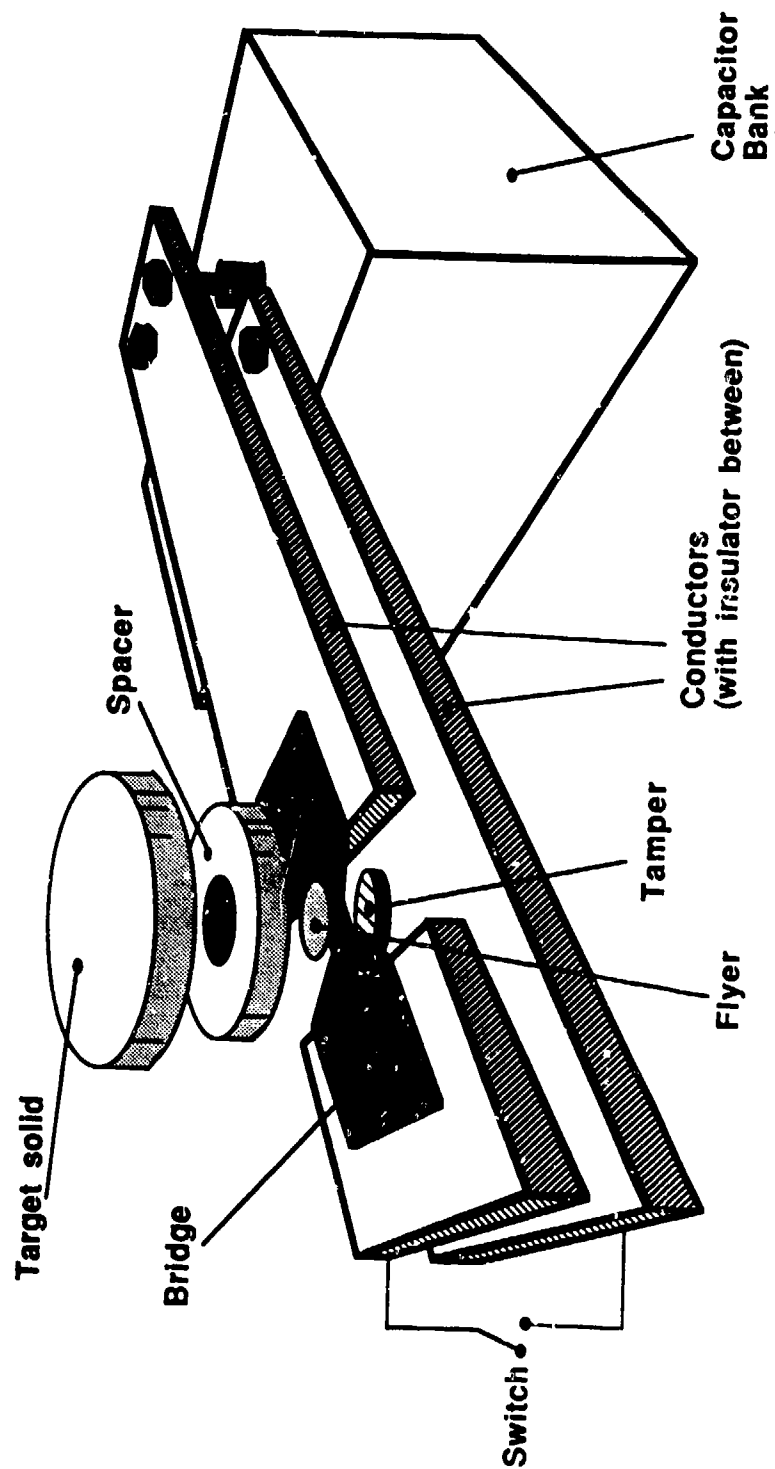
Boomer Set Up
(very large scale FPG)

Capacitor Bank

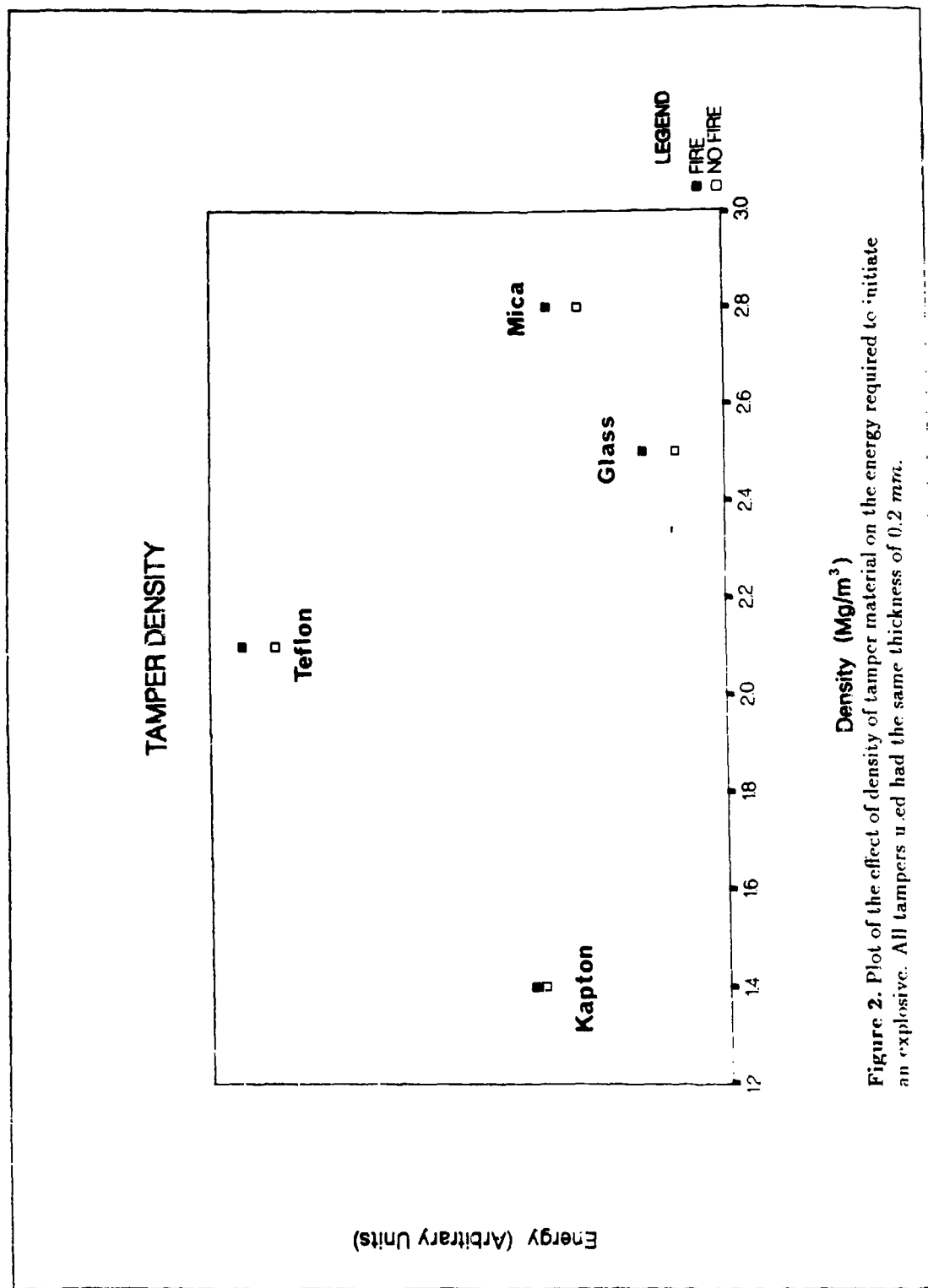Conductors
(with insulator between)

Tamper

Flyer

Spacer

Target solid

Bridge

Switch

FIGURE 1B

TAMPER DENSITY

Figure 2. Plot of the effect of density of tamper material on the energy required to initiate an explosive. All tampers u.ed had the same thickness of 0.2 mm.
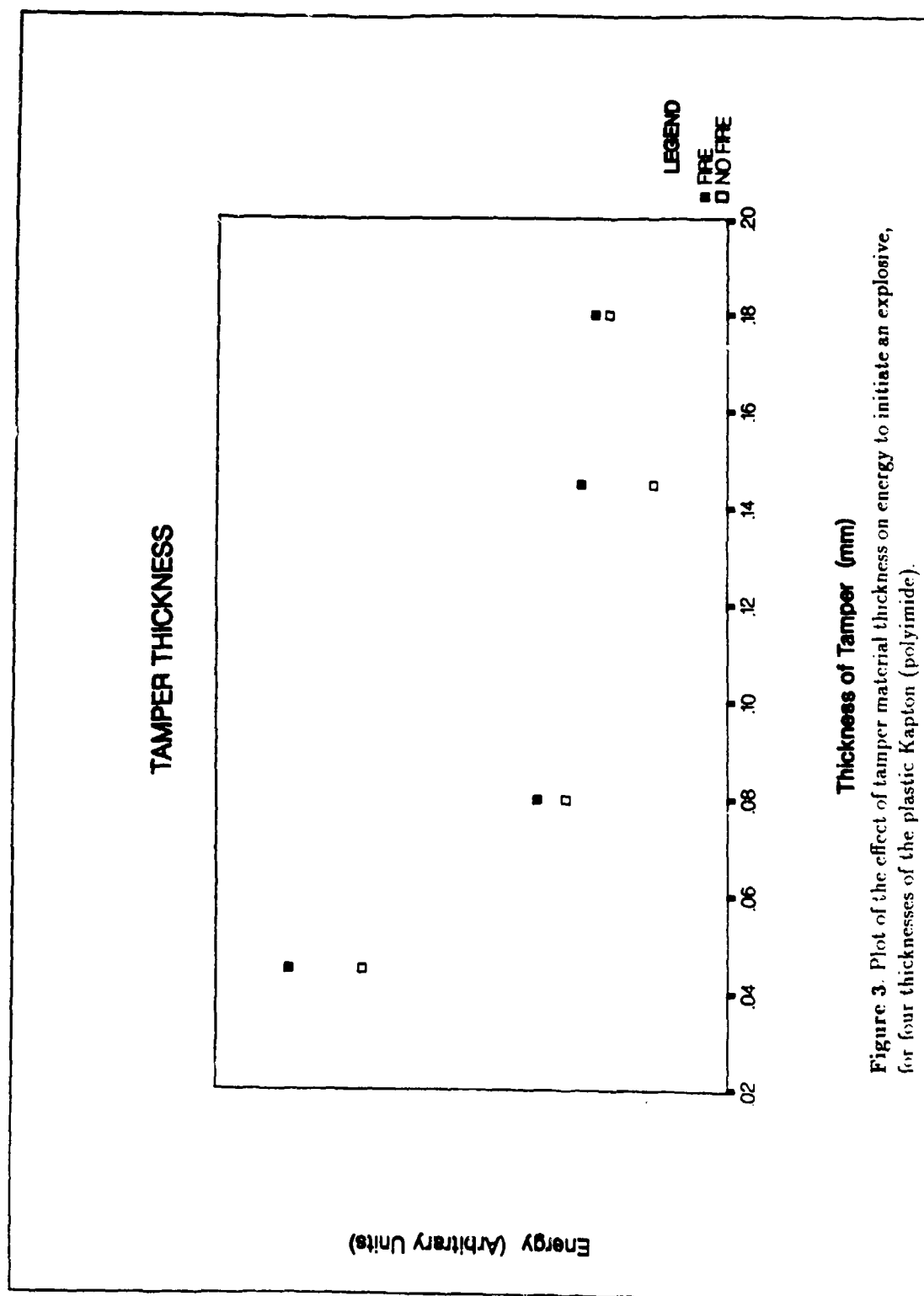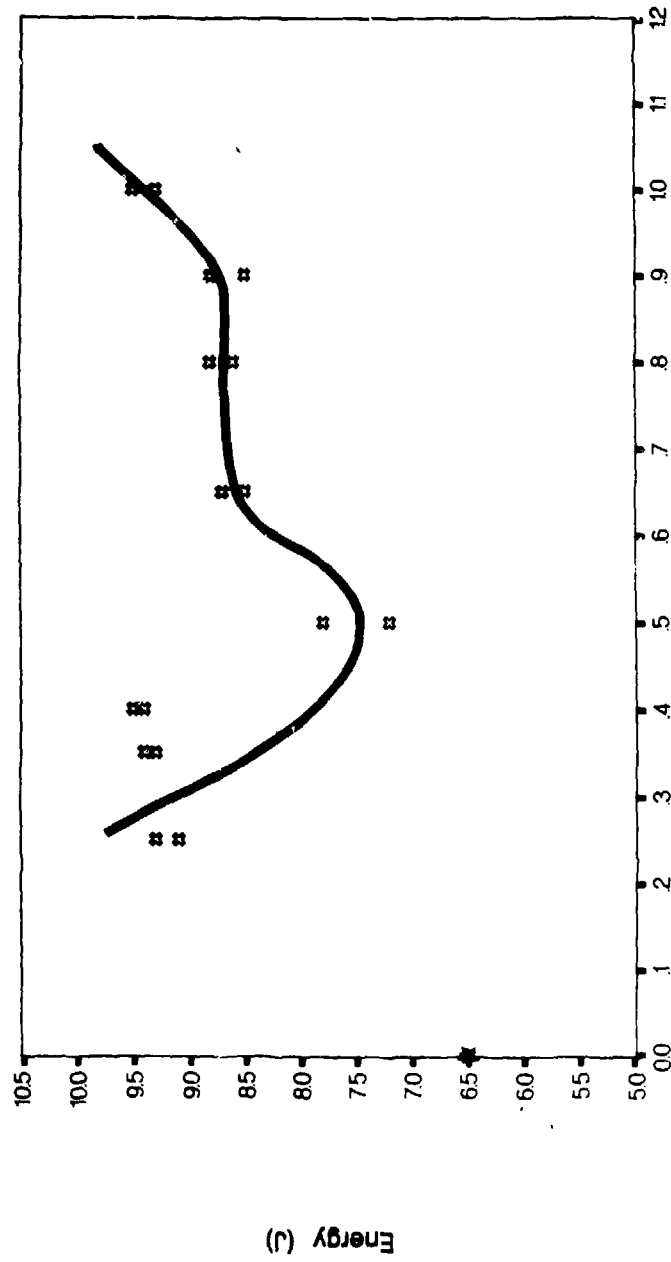
TAMPER THICKNESS

Thickness of Tamper (mm)

Energy (Arbitrary Units)

LEGEND
■ FIRE
□ NO FIRE

Figure 3. Plot of the effect of tamper material thickness on energy to initiate an explosive, for four thicknesses of the plastic Kapton (polyimide).

ENERGY TO INITIATE PETN vs BARREL LENGTH

Barrel Length (mm)

Figure 4. Plot of the dependence of the energy required to initiate an explosive on the length of the barrel in the FPG. The bars indicate the range over which both fires and no fires occurred. The range is thought to be due to inconsistent functioning of the spark gap switch used. The extrapolation to obtain E_o is shown.
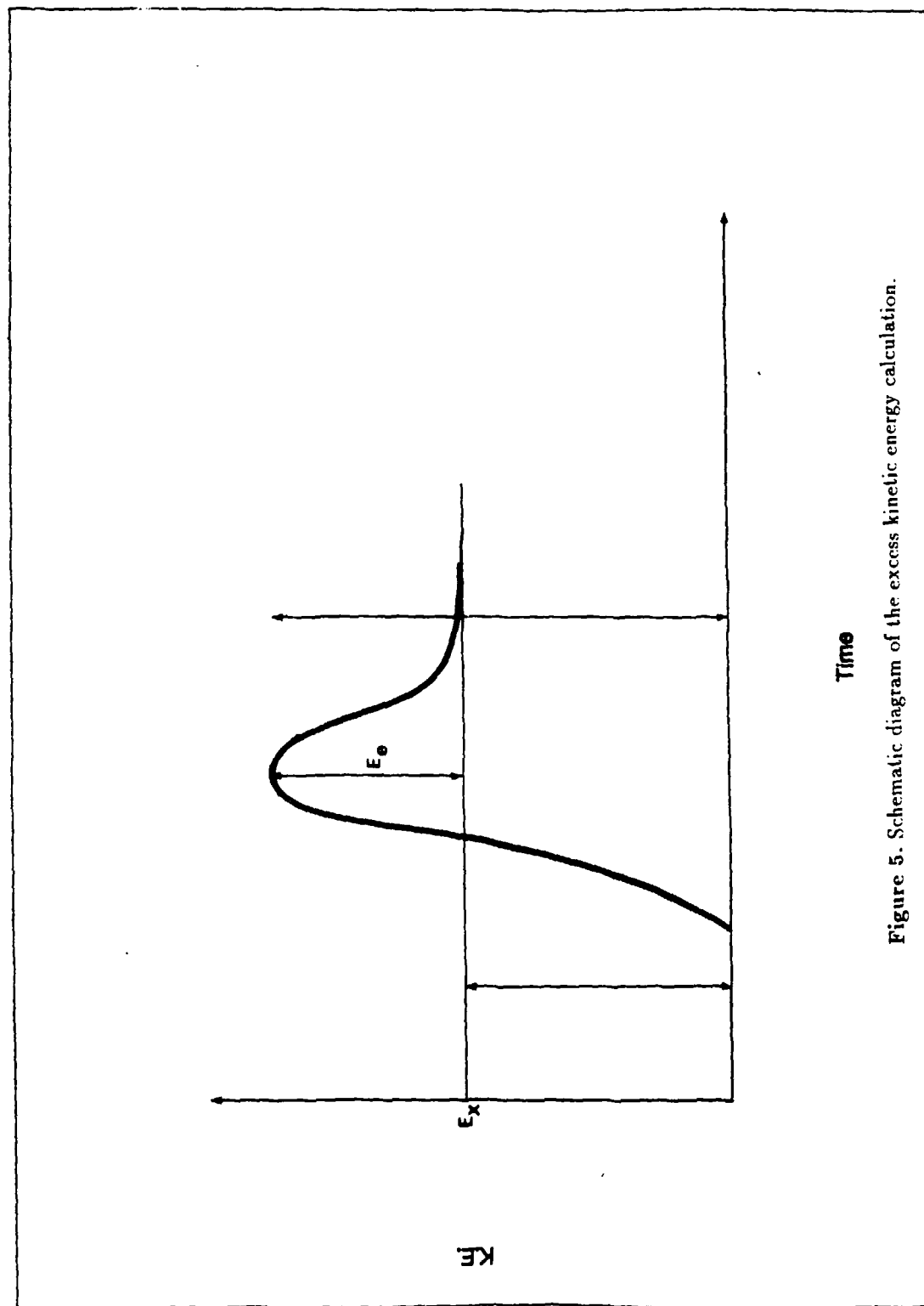
Figure 5. Schematic diagram of the excess kinetic energy calculation.
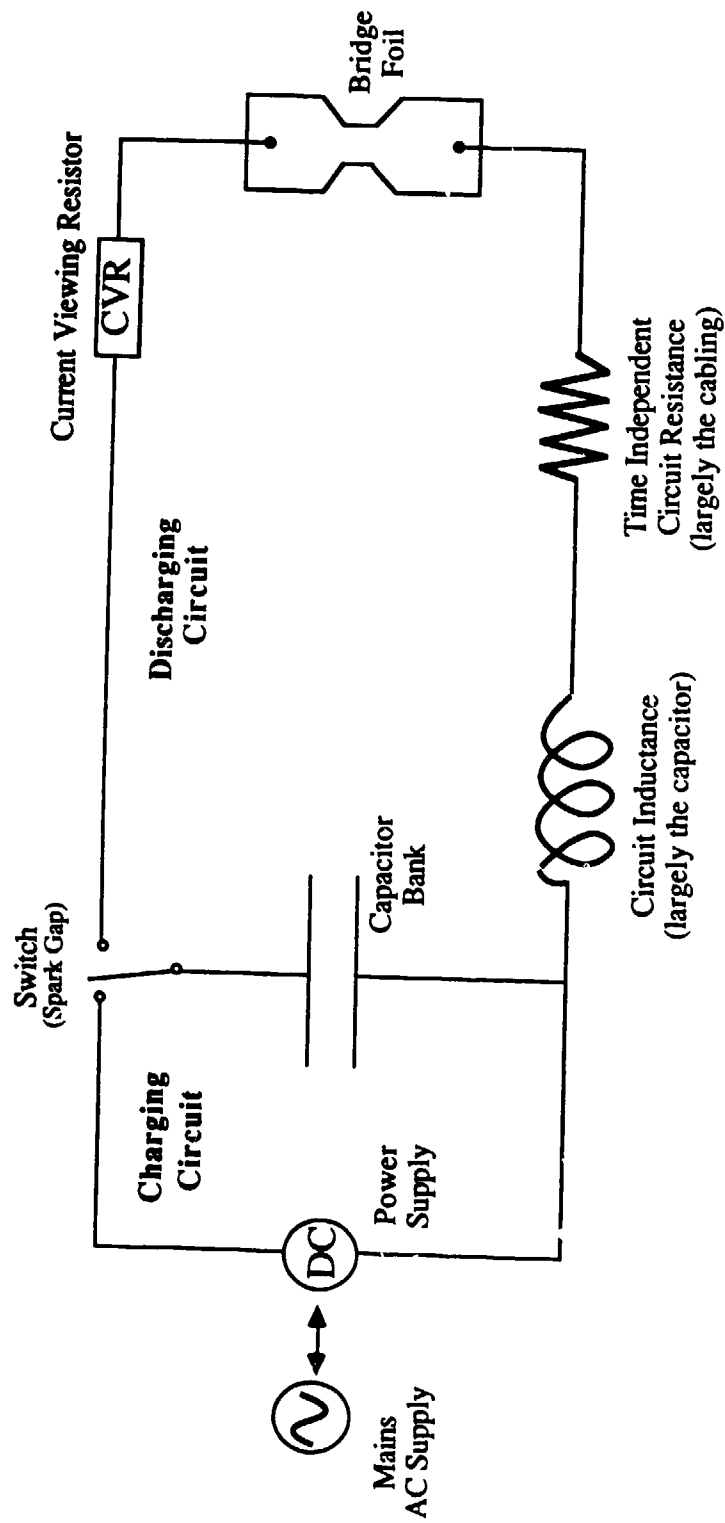
Schematic Flying Plate Generator Circuit

Figure 8. Schematic diagram of the electrical circuit of the FPG.
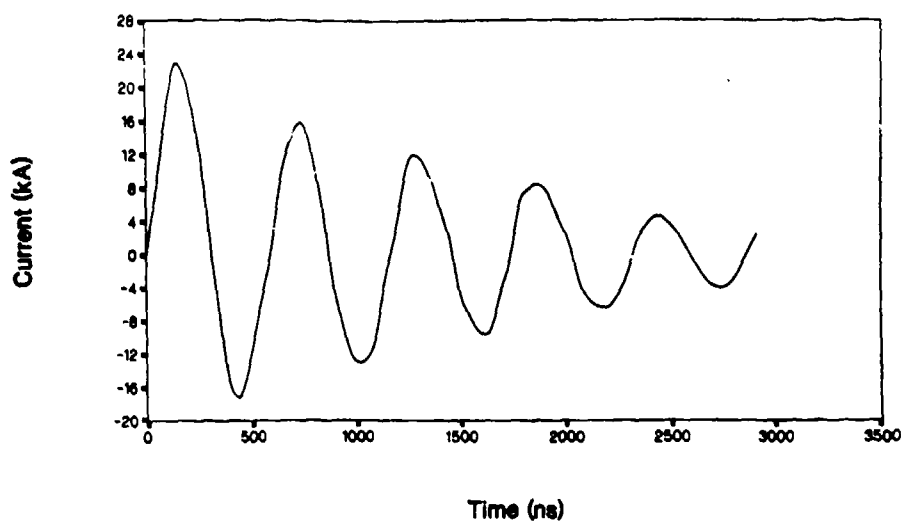
Current Trace for FPG Ringdown

Time (ns)

Figure 7. (a) Current trace of a typical ringdown at 9 kV (the bridge foil is replaced with a short). Note the exponentially-damped sinusoid nature of the trace. From the period and the heights of the peaks, it is possible to infer the resistance and inductance of the $R - L - C$ circuit.
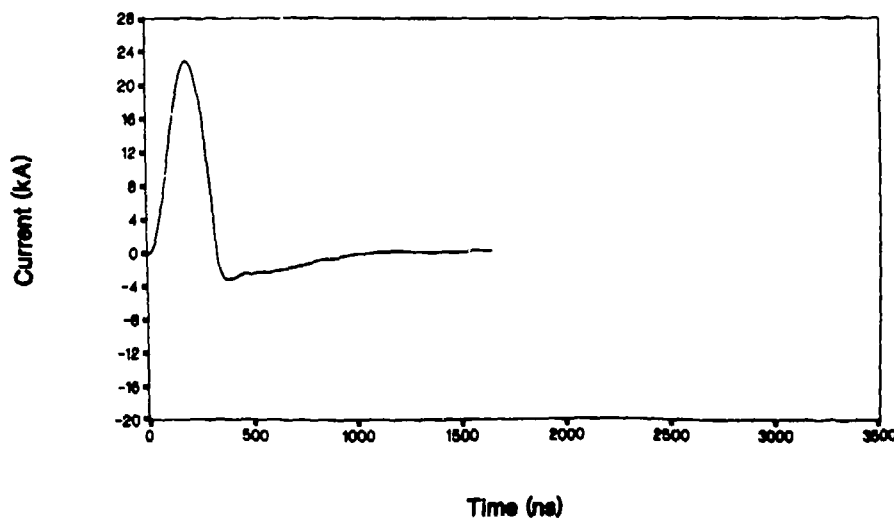
Current Trace for Bridge Burst

Time (ns)

Figure 7. (b) Current trace of a bridge burst at 9 kV, for a 3 mm wide copper bridge (the lands of the bridge are about 15x15 mm). Note the similarity to (a) up until about the first peak, which implies that the circuit is affected at this time by the bridge material vaporising.

DOCUMENT CONTROL DATA SHEET

REPORT NO.	AR NO.	REPORT SECURITY CLASSIFICATION
MRL-R-1133	AR-005-250	Unclassified

TITLE

An exploding foil flying plate generator

AUTHOR(S)	CORPORATE AUTHOR
D.D. Richardson	Materials Research Laboratory, DSTO
E.D. Northeast and	PO Box 50,
P.F.X. Ryan	Ascot Vale, Victoria 3032

REPORT DATE	TASK NO.	SPONSOR
August 1988	DST 85/159	DSTO

FILE NO.	REFERENCES	PAGES
G6/4/8-3425	28	37

CLASSIFICATION/LIMITATION REVIEW DATE	CLASSIFICATION/RELEASE AUTHORITY
	Chief, Explosives Division
	MRL

SECONDARY DISTRIBUTION

Approved for public release

ANNOUNCEMENT

Announcement of this report is unlimited

KEYWORDS		
Exploding foil	High Velocity	Flying plate generator
Shock waves	Explosive initiation	

SUBJECT GROUPS   0079A

ABSTRACT

This paper reports on work done at MRL to generate and use high velocity flying plates. The plates are generated by the pressure from an electrically burst metal foil. We examine some of the important design characteristics of the flying plate generator. We list some possible applications of the method as it applies to shock waves in materials. A discussion of phenomena which have been discovered by using plate impact on a High Explosive to indirectly monitor flying plate velocity is presented.